# Improvement Transient Stability of Fixed Speed Wind Energy Conversion System by Using Transformer-Type Superconducting Fault Current Limiter

**Ali Azizpour[1], Seyed Etezad Moghimi[2], Sajad Dadfar[3]**

[1] *Department of Electrical Engineering, Mazandaran university of Science and Technology, Behshahr, Iran*
[2,3] *Iran Power Generation, Transmission and Distribution Management Company (TAVANIR), Iran*

---

**Abstract** - *The wind turbine generation system (WTGS) is one of the representative renewable energy systems. With the rapid development of WTGS and its increased capacity, the level of short circuit current will increase in distribution systems. The application of the Superconducting Fault Current Limiter (SFCL), would not only reduce the level of the short circuit current but also offer a reliable interconnection to the network. The transformer-type superconducting fault current limiter (SFCL) is one of the fault current limiters, and has many advantages such as design flexibility. In this paper, the effect of transformer -type SFCL on transient behavior of grid connected to WTGS is studied. The WTGS is considered as a fixed-speed system, equipped with a squirrel-cage induction generator. The drive-train is represented by two-mass model. The simulation results show that the transformer -type SFCL not only limits the fault current but also can improve the dynamic performance of the WTGS.*

**Key Words: Wind Turbine Integration, Fixed Speed Wind Turbine, Induction Generator, Transformer-Type SFCL, Transient Stability**

## 1.INTRODUCTION

There are promising reasons that future power grids will be different compared to current power grids due to integration of renewable energy resources which require new controlling, monitoring and protection models [1-2] .Energy and environmental issues have become one of the main challenges facing the world. Concerning about environmental pollution and a possible energy shortage, the capacities of renewable energy generation systems, are being expanded. Generally, renewable energy resources provide both electric utilities and customers with a lot of benefits including: high quality electricity, emission reduction, and so on [3-6]. By increasing development of robotics field using renewable energy in this field also attracts a lot of researchers' attention [7-10]. Free and clean renewable energy resources such as solar photovoltaic and wind generation offer flexibility to the power network and are the key players in reducing operating cost and emissions of the system [11-13]. However, due to their intermittency and uncertainty, integrating them into the power system is challenging and complicated [14-15]. Each renewable energy sources have different challenges. Some photovoltaic systems challenges are their optimum tilt angle [16] and effect of temperature on PV panels[17]. Indeed, balancing supply and demand in power systems including large amount of renewable energy penetration requires flexible renewable energy resources [18-27].

The WTGS is one of the representative renewable energy systems. Wind energy conversion systems have two types: fixed and variable speed systems. As a simple conversion system, the fixed speed system is still applied at electric power industry. It is necessary to research power flow and transient stability of distribution system with wind turbine generators [28-30].

The connection of wind turbines to the grid causes the fault current level increase beyond capabilities of existing equipment in some points of grids. This not only might damage the series equipment but also can cause negative effect on WTGS with respect to voltage stability [31].

Increasing fault currents often requires the costly replacement of substation equipment or the imposition of changes in the configuration that may lead to decreased operational flexibility and lower reliability. An alternative approach to reduce the fault current is the application of Fault Current Limiters (FCLs). Their application allows equipment to remain in service, even if the fault current exceeds its rated peak and short time withstand current [32-33]. Since the voltage sag during the fault is proportional to the short circuit current, an effective fault current limiter connected to the WTGS not only limits the large fault current but also improves the voltage stability of WTGS [34]. In

recent years, various types of FCL such as, solid state FCL, resonant circuit and SFCL (Superconducting Fault Current Limiter) have been proposed and developed [35]. SFCL offers a solution to limit fault current with many significant advantages. The application of the SFCL would not only decrease the stress on device but can also improve reliability, improve power quality, limit the inrush current of transformers, reduce the transient recovery voltage (TRV) across the CBs and improve transient stability of power systems by reducing the fault current. There are different types of SFCLs which are based on different superconducting materials and designs such as, flux-lock, transformer, resistive and bridge-types SFCL [36-38]. The transformer-type SFCL has zero impedance under normal conditions and large impedance under fault conditions (the same as other FCLs) [39-43]. But, it has significant advantages as follow:

- large design flexibility of the current limiting device,
- isolation between the current limiting device and the power transmission line,
- reduction of heat loss of the current limiting device
- prevention from instantaneously deep voltage drop during fault

This characteristic of the transformer-type SFCL suppresses the instantaneous voltage drop and it is able to improve transient behavior of WTGS during fault. In this paper, the effect of transformer-type SFCL on transient behavior of WTGS is studied. The WTGS is considered as a fixed-speed system, equipped with a squirrel-cage induction generator. The drive-train is represented by two-mass model. The simulation results show that the transformer-type SFCL can improve the dynamic performance of the WTGS.

## 2. Transformer-Type Fault Current Limiter

### 2.1. Power Circuit of Transformer-Type SFCL

The transformer-type SFCL is shown in Fig. 1. This type of FCL basically consists of a transformer in series with the line and a resistive superconducting current limiting device connected to the secondary winding of the series transformer (T).

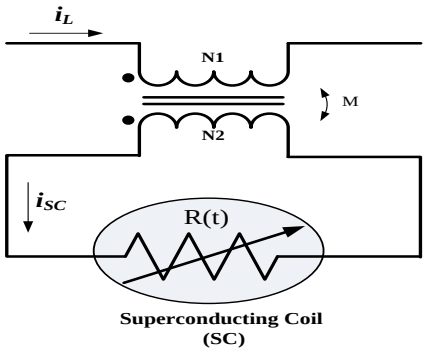


Fig. 1: Transformer-type SFCL

### 2.2. Characteristic of Transformer-Type SFCL During Fault

The circuit shown in Fig. 2 has been used for analytical studies. The source impedance has been modeled by $z_s = r_s + j\omega L_s$ . The impedance, $z_L = r_L + j\omega L_L$ presents the line and load impedance.

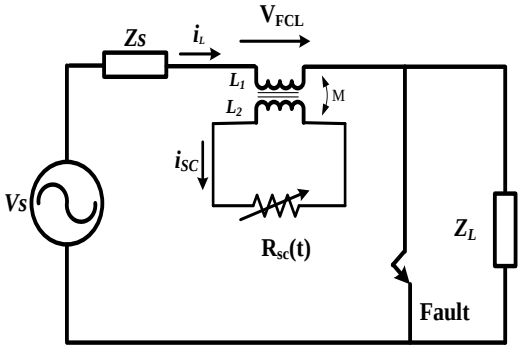


Fig. 2: Circuit topology for analytical analysis

$L_1$ and $L_2$ presents the primary and secondary leakage inductance of transformer, M is the mutual inductance between the primary and secondary winding and $R_{SC}(t)$ is the resistance of the superconducting current limiting device. $i_L$ and $i_{SC}$ presents the line current and superconducting current limiting device currents, respectively. In this paper, the time-dependent resistance of the superconducting current limiting device during its S-N transition (transition from Superconducting state to Normal-conducting state) is represented by an exponential function as following expression:

$$R_{SC}(t) = 0 \qquad t<t_f \qquad (1)$$

$$R_{SC}(t)=R_m(1-e(t-t_1)/T) \qquad t\geq t_f \qquad (2)$$

Rm is the maximum value of the superconducting current limiting device current limiting device resistance; T is the time constant of the resistance

increase. The characteristic of the SC device used for analysis is shown in Fig. 3.

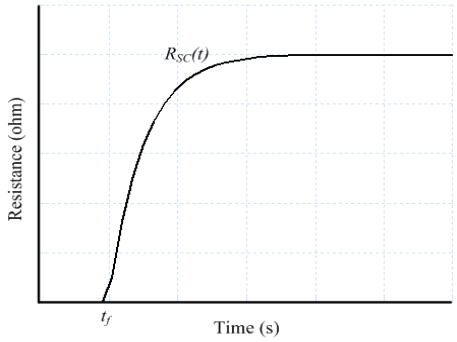


Fig. 3: Resistance of superconducting current limiting device during transition

Under the normal operating condition, the transformer-type SFCL shows very low impedance because the resistance of the superconducting current limiting device is zero (RSC(t)=0). But, when fault occurs (t=tf) in the line, large fault current flows through the transformer. This will cause the current through the superconducting current limiting device, to increase beyond its critical level and the resistance of superconducting current limiting device is increased during fault. As a result, the transformer-type SFCL will limit the fault current at determined value as shown in Fig. 4.

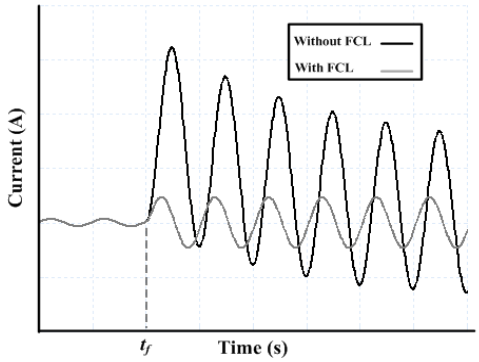


Fig. 4: Fault current during fault and normal operation with using transformer-type SFCL

## 3.Modeling of Fixed Speed Wind Turbine

Fixed-speed wind turbine utilizes squirrel cage IG directly connected to the power grid and, therefore, the wind turbine rotor speed is fixed and determined by the frequency of the supply grid, the gear ratio and the IG design. IGs always need to absorb a particular amount of reactive power. Thus, they generally have fixed reactive power support devices [44].

### 3.1. Wind Speed Model

One approach to model a wind speed sequence is to use measurements. A more flexible approach is to use a wind speed model that can generate wind speed sequences with characteristics to be chosen by the user. As shown in Fig. 5, wind speed is modeled as the sum of vwa(t) base wind speed , vwg(t) gust wind speed , vwr(t) ramp wind speed and vwt(t) noise wind speed [45]. According to these four wind speeds, the adopted wind speed model for a single wind turbine is, as follows:

$$v_w(t) = v_{wa}(t) + v_{wr}(t) + v_{wg}(t) + v_{wt}(t) \quad (3)$$

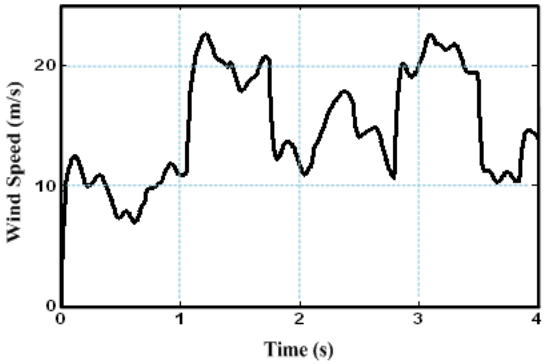


Fig. 5: Wind Speed Model

### 3.2. Wind Turbine Model In general, the relation between described, as follow [46]:

$$P_{wt} = \frac{\rho}{2} . A_{wt} C_p(\lambda,\theta) v_w^3 \quad (4)$$

where, Pwt is the power extracted from the wind, ρ is the air density, vw is the wind speed, CP is the performance coefficient or power coefficient, λ is the tip speed ration, Awt = πR2 is the area covered by the wind turbine rotor, R is the radius of the tip speed ration and λ is defined, as follows:

$$P_{wt} = \frac{R_{\omega r}}{v_w} \quad (5)$$

where, ωr is the angular mechanical speed. The performance coefficient is different for each turbine and is relative to the tip speed ratio λ and pitch angle β. In this paper, the Cp is, as follows:

$$C_p = \frac{1}{2}(\lambda - 0.022\beta^2 - 5.6)\, e^{-0.17\lambda} \quad (6)$$

The CP - λ curves are shown in Fig. 6 for different values of β.

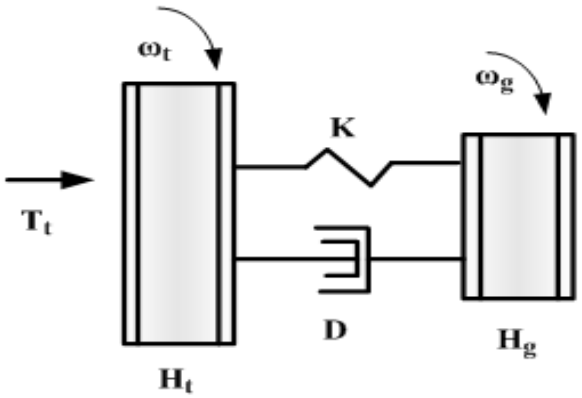


Fig. 6: CP- λ curves for different pitch angles

### 3.3. Shaft Model/ Drive Train System

The shaft model of the wind turbine is described by the two-mass model as shown in Fig. 7 and defined by the following equation:

$$\frac{\partial\theta}{\partial t} = \omega_t - \omega g \quad (7)$$

$$\frac{\partial\omega_t}{\partial t} = \frac{1}{2H_t}(T_t - K_s\theta_s + D(\omega_g - \omega_t)) \quad (8)$$

$$\frac{\partial\omega_g}{\partial_t} = \frac{1}{2H_g}(-T_e + K_s\theta_s - D(\omega_g - \omega_t)) \quad (9)$$

Where,

*Tt* : the mechanical torque referred to the generator side,

*Te*: the electromagnetic torque,

*Ht* : the equivalent turbine-blade inertia,

*Hg*: the generator inertia,

*ωt*: the turbine's rotational speed,

*ωg*: the generator's rotational speed,

*K*: the shaft stiffness

*D*: the damping constant

*Θs*: the angular displacement between the ends of the shaft

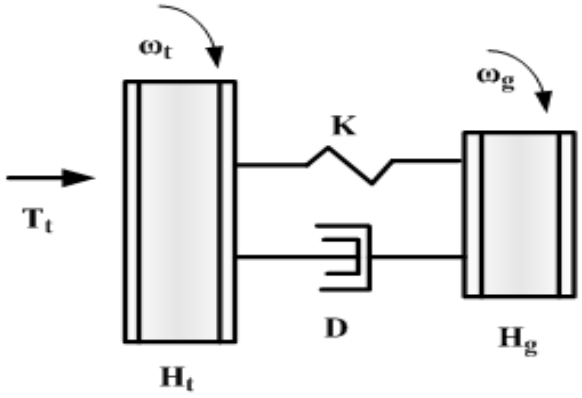


Fig. 7: Two mass model of wind turbine train

### 3.4. Induction Generator Model

The PSCAD/EMTDC software library provides a standard model for the induction generator, represented by a standard seventh-order model in a d-q reference frame. This model is used in this paper.

## 4. Stability Analysis

The concept of the induction generator stability can be further explained by using the electrical torque versus rotor speed curve of an induction generator. In order to obtain a mathematical relationship between electrical torque and rotor speed, the steady-state equivalent circuit of an induction generator shown in Fig. 8 is used [47-49].

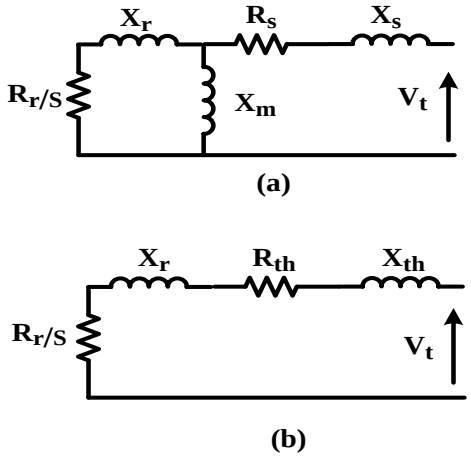


Fig. 8: Steady-state equivalent circuit of induction generator (a), complete model and (b) Thevenin model.

The electrical torque, Te can be calculated, as follows:

$$T_e = \frac{R_r}{S} I_r^{\,2} = \frac{R_r}{s} \frac{V_{th}^{\,2}}{(R_{th} + R_r / s)^2 + (X_{th} + X_r)^2} \quad (10)$$

When the induction machine operates as a generator, the mechanical torque is negative. Therefore, the electrical-mechanical equilibrium equation of an induction generator can be written, as follows:

$$\frac{d\omega_r}{dt} = \frac{(T_e - T_m)}{2H} \qquad (11)$$

where, H is the inertia constant. From Eq. (11), two equilibrium points, where the electrical torque is equal to the mechanical torque, can be found. Using FCL has advantages as follows:

- The fault current is limited and voltage sag is prevented at the terminal voltage of induction generator ($V_t$). According to Eq. (10), the electrical torque is proportional to the square of the terminal voltage. Therefore, FCL prevents from the decreasing electrical torque and accelerating the induction generator.

- FCL prevents from increasing speed independent of fault clearing time. According Eq. (10), the electrical torque is inversely proportional to slip and rotor speed. Therefore, FCL prevents from decreasing electrical torque and accelerating induction generator.

## 5. Simulation Results

A single line diagram of the simulated power system with transformer-type SFCL is shown in Fig. 9. The parameters of this system are listed in table I in appendix A. A 3-phase short circuit fault is simulated on line 2which starts at t=10s. After 200ms, the circuit breaker isolated the faulted line. The simulations have been carried out by PSCAD/EMTDC for two cases, as follows:

- Case A: Without using any FCL in the system
- Case B: By using the transformer-type SFCL

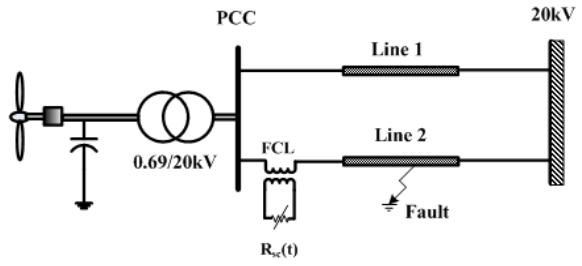


Fig. 9: Simulated power system with transformer-type SFCL

Fig. 10 shows the rms value of the PCC voltage in the both cases (A) and (B). It can be observed that the PCC voltage decreases to zero in case A, approximately. The transformer-type SFCL not only decreases the voltage sag to 0.95 pu, but also prevents from instantaneous voltage sag in fault instant. Fig. 11 shows the total active power generated by the induction generator and the grid. During the fault (10s<t<10.2s), the active power generated by the induction generator is increased by using the transformer-type SFCL. Fig. 12 shows the total reactive power exchanged between the induction generator and the grid. After the fault has cleared (at t = 10.2 s), the absorbing reactive power from the grid is significantly reduced. However, the reactive power absorbed by the induction generator is reduced, in case B. Figures 13 and 14 show the rotor speed of the induction generator, and the electrical torque, respectively. As shown in Fig. 13, the generator rotor-speed swing is reduced in case B. These results show that transformer-type SFCL can provide an effective damping to the post-fault oscillations of the induction generator. As shown in Fig. 14, the variation of the electrical torque is reduced in case B. Because the transformer-type SFCL in prevents an instantaneous voltage sag during fault. The transformer-type SFCL is very effective in suppressing the variations of the electrical torque during fault, but it results in swings after fault clearing.

Fig. 15 shows the rotor current of induction generator. In both figures, the amplitude of rotor currents is reduced in case B. However, the rotor current transients are significantly reduced in fault instant and after fault clearing.

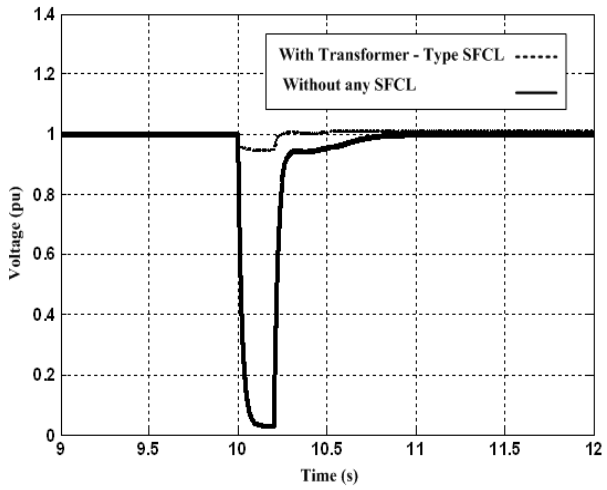


Fig. 10: Effect of transformer-type SFCL on PCC voltage

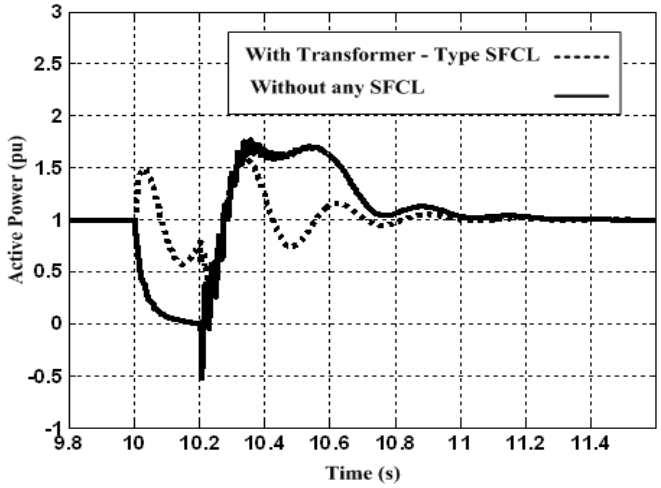


Fig. 11: Active power of induction generator during fault

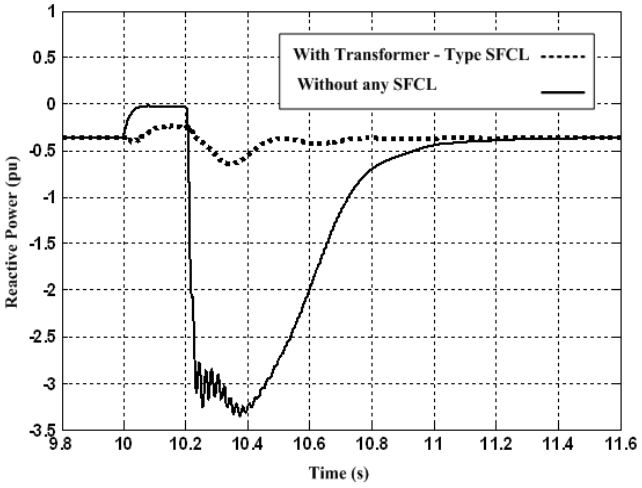


Fig. 12: Reactive power of induction generator during fault

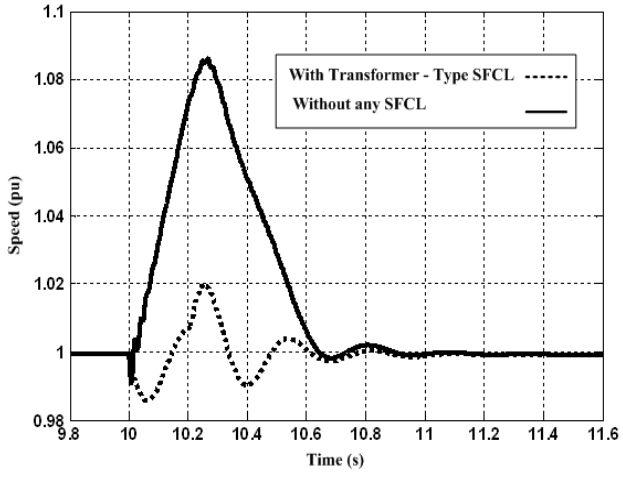


Fig. 13: Rotor speed of induction generator during fault

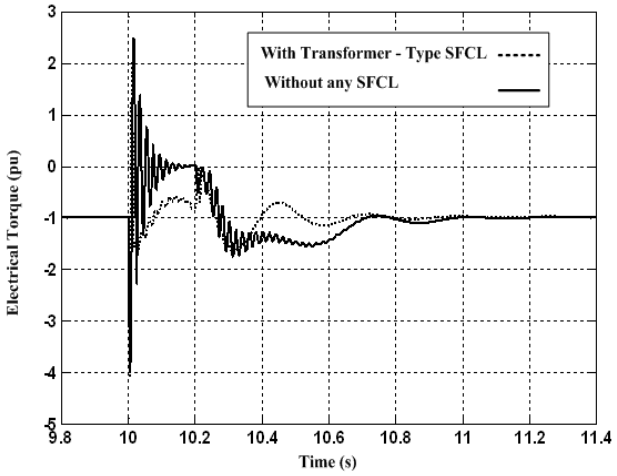


Fig. 14: Electrical torque of induction generator during fault

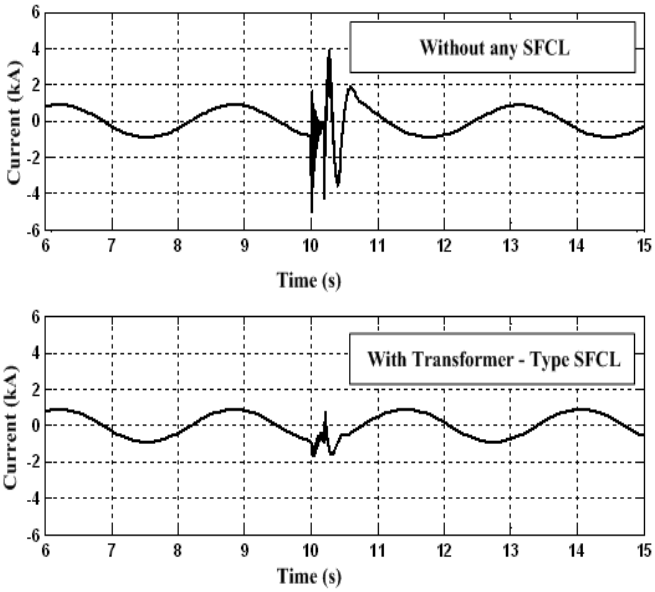


Fig. 15: Electrical torque of induction generator during fault

## 6. CONCLUSION

In this paper, the effect of the transformer-type SFCL in transient performance of fixed speed turbines has been studied based simulation by PSCAD/EMTDC. The simulation results show that the transformer - type SFCL not only limits the fault current but also suppresses the voltage drop and improves generator stability. Also, the oscillation of active and reactive powers, electrical torque and stator and rotor currents are reduced effectively during fault.

Appendix

Table 1: Parameters of test system

| Parameters | | Value |
|---|---|---|
| grid | Supply | 20 kV |
| | Frequency | 50Hz |
| | Step down transformer | .69kV/20 kV |
| line | R | 0.1(Ω/km) |
| | X | 0.2(Ω/km) |
| | Length of $Line_1$ | 20 km |
| | Length of $Line_2$ | 20 km |
| Induction Generator | Power | 1MW |
| | Voltage | 690 V |
| | Frequency | 50 Hz |
| | Number of poles | 4 |
| | Stator resistance | 0. 00577 Ω |
| | Stator reactance | 0.0782 Ω |
| | Rotor resistance | 0. 0161 Ω |
| | Rotor reactance | 0.1021 Ω |
| | Magnetizing reactance | 2.434 Ω |
| FCL | SC resistance | 10 Ω |

## REFERENCES

[1] A. Ghasemkhani, H. Monsef, A. Rahimi-Kian, and A. Anvari- Moghaddam, "Optimal Design of a Wide Area Measurement System for Improvement of Power Network Monitoring Using a Dynamic Multi Objective Shortest Path Algorithm," IEEE Syst. J., vol. PP, no. 99, pp. 1–12, 2015.

[2] A. Ghasemkhani, A. Anvari-Moghaddam, J. M. Guerrero, and B. Bak-Jensen, "An Efficient Multi-objective Approach for Designing of Communication Interfaces in Smart Grids," Proceedings of IEEE PES Innovative Smart Grid Technologies, Ljubljana, Slovenia (ISGT Europe 2016), Oct. 2016.

[3] L. A. Duffaut Espinosa, M. Almassalkhi, P. Hines, S. Heydari, and J. Frolik, "Towards a Macromodel for Packetized Energy Management of Resistive Water Heaters," in Conference on Information Sciences and Systems, Mar. 2017.

[4] F. Farmani, M. Parvizimosaed, H. Monsef, A. Rahimi-Kian, A conceptual model of a smart energy management system for a residential building equipped with CCHP system, In International Journal of Electrical Power & Energy Systems, Volume 95, 2018, Pages 523-536.

[5] M. Parvizimosaed, F. Farmani, H. Monsef, A. Rahimi-Kian, A multi-stage Smart Energy Management System under multiple uncertainties: A data mining approach, In Renewable Energy, Volume 102, Part A, 2017, Pages 178-189.

[6] Parvizimosaed M, Farmani F, Anvari-Moghaddam A. Optimal energy management of a micro-grid with renewable energy resources and demand response. J Renew Sustain Energy 2013;5:053148.

[7] Gharghabi, S., Azari, B., Shamshirdar, F. and Safabakhsh, R., "Improving person recognition by weight adaptation of soft biometrics," In Computer and Knowledge Engineering (ICCKE), 2016 6th International Conference on(pp. 36-40). IEEE.

[8] Gharghabi, S. and Safabakhsh, R., "Person recognition based on face and body information for domestic service robots," In Robotics and Mechatronics (ICROM), 2015 3rd RSI International Conference on (pp. 265-270). IEEE.

[9] Andani, M.T. and Ramezani, Z., 2017. Robust Control of a Spherical Mobile Robot.

[10] Pourseif, T., Andani, M.T., Ramezani, Z. and Pourgholi, M., 2017. Model Reference Adaptive Control for Robot Tracking Problem: Design & Performance Analysis. International Journal of Control Science and Engineering, 7(1), pp.18-23.

[11] S. Aznavi, P. Fajri, M. Benidris and B. Falahati "Hierarchical Droop Controlled Frequency Optimization and Energy Management of a Grid-Connected Microgrid," presented at 2017 IEEE Conference on Technologies for Sustainability, (SusTech), Phoenix, AZ, 2017.

[12] Yousefpour, Kamran. "Placement of Dispersed Generation with the Purpose of Losses Reduction and Voltage Profile Improvement in Distribution Networks Using Particle Swarm Optimization Algorithm." Journal of World's Electrical Engineering and Technology 2322 (2014): 5114.

[13] Yousefpour, Kamran, Seyyed Javad Hosseini Molla, and Seyyed Mehdi Hosseini. "A Dynamic Approach for

Distribution System Planning Using Particle Swarm Optimization." International Journal of Control Science and Engineering 5.1 (2015): 10-17.

[14] Amini, Mahraz, and Mads Almassalkhi. "Investigating delays in frequency-dependent load control." Innovative Smart Grid Technologies-Asia (ISGT-Asia), 2016 IEEE. IEEE, 2016.

[15] Jafarishiadeh, Seyyedmahdi, and Mahraz Amini. "Design and comparison of axial-flux PM BLDC motors for direct drive electric vehicles: conventional or similar slot and pole combination." International Journal of Engineering Innovations and Research 6.1 (2017): 15.

[16] H. Pourgharibshahi, M. Abdolzadeh, and R. Fadaeinedjad, "Verification of computational optimum Tilt angles of a photovoltaic module using an experimental photovoltaic system," Environmental Progress & Sustainable Energy, vol. 34, no. 4, pp. 1156-1165, 2015.

[17] A. Rouholamini, H. Pourgharibshahi, R. Fadaeinedjad, and M. Abdolzadeh, "Temperature of a photovoltaic module under the influence of different environmental conditions–experimental investigation," International Journal of Ambient Energy, vol. 37, no. 3, pp. 266-272, 2016.

[18] S.M.M. H.N, S. Heydari, H. Mirsaeedi, A. Fereidunian, A.R. Kian," Optimally operating microgrids in the presence of electric vehicles and renewable energy resources," Smart Grid Conference (SGC), Iran, Dec., 2015.

[19] Imani, SM Hossein, S. Asghari, and M. T. Ameli. "Considering the load uncertainty for solving security constrained unit commitment problem in presence of plug-in electric vehicle." Electrical Engineering (ICEE), 2014 22nd Iranian Conference on. IEEE, 2014.

[20] Imani, M. Hosseini, Payam Niknejad, and M. R. Barzegaran. "The impact of customers' participation level and various incentive values on implementing emergency demand response program in microgrid operation." International Journal of Electrical Power & Energy Systems 96 (2018): 114-125.

[21] F. Rahmani, F. Razaghian, and A. Kashaninia, "Novel Approach to Design of a Class-EJ Power Amplifier Using High Power Technology," World Academy of Science, Engineering and Technology, International Journal of Electrical, Computer, Energetic, Electronic and Communication Engineering, vol. 9, pp. 541-546, 2015.

[22] F. Rahmani, F. Razaghian, and A. Kashaninia, "High Power Two-Stage Class-AB/J Power Amplifier with High Gain and Efficiency," Journal of Academic and Applied Studies (JAAS), vol. 4, pp. 56-68, 2014.

[23] P. Niknejad, T. Agarwal, and M. Barzegaran, "Using gallium nitride DC-DC converter for speed control of BLDC motor," in Electric Machines and Drives Conference (IEMDC), 2017 IEEE International, 2017, pp. 1-6.

[24] T. Agarwal, D. Kumar, and N. R. Prakash, "Prolonging network lifetime using ant colony optimization algorithm on LEACH protocol for wireless sensor networks," Recent Trends in Networks and Communications, pp. 634-641, 2010.

[25] Parvizimosaed M, Farmani F, Rahimi-Kian A, Monsef H. A multi-objective optimization for energy management in a renewable micro-grid system: a data mining approach. J Renew Sustain Energy 2014;6:023127.

[26] A. Ameli, M. Farrokhifard, A. Shahsavari, A. Ahmadifar and H. A. Shayanfar, "Multi-objective DG planning considering operational and economic viewpoints," 2013 13th International Conference on Environment and Electrical Engineering (EEEIC), Wroclaw, 2013, pp. 104-109.

[27] A. Ameli, A. Ahmadifar, M. H. Shariatkhah, M. Vakilian, and M. R. Haghifam. "A dynamic method for feeder reconfiguration and capacitor switching in smart distribution systems." International Journal of Electrical Power & Energy Systems, vol. 85, pp. 200-211, 2017.

[28] D. Gautam, V. Vittal, and T. Harbour, "Impact of increased penetration of DFIG-based wind turbine generators on transient and small signal stability of power systems," Power Systems, IEEE Transactions on, vol. 24, pp. 1426-1434, 2009.

[29] J. M. Rodríguez, J. L. Fernández, D. Beato, R. Iturbe, J. Usaola, P. Ledesma, et al., "Incidence on power system dynamics of high penetration of fixed speed and doubly fed wind energy systems: study of the Spanish case," Power Systems, IEEE Transactions on, vol. 17, pp. 1089-1095, 2002.

[30] W.-J. Park, B. C. Sung, and J.-W. Park, "The effect of SFCL on electric power grid with wind-turbine

generation system," Applied Superconductivity, IEEE Transactions on, vol. 20, pp. 1177-1181, 2010.

[31] CIGRE WG A3.10: "Fault Current Limiters in High Electrical Medium and Voltage Systems", CIGRE Technical Brochure, No.239, 2003.

[32] CIGRE WG A3.10: "Fault Current Limiters Report on the Activities of CIGRE WG 3.16", CIGRE Technical Brochure, 2006.

[33] M. Firouzi, G. Gharehpetian, and M. Pishvaei, "A dual-functional bridge type FCL to restore PCC voltage," International Journal of Electrical Power & Energy Systems, vol. 46, pp. 49-55, 2013.

[34] H. G. Sarmiento, R. Castellanos, G. Pampin, C. Tovar, and J. Naude, "An example in controlling short circuit levels in a large metropolitan area," in Power Engineering Society General Meeting, 2003, IEEE, 2003.

[35] S.-Y. Kim, J.-O. Kim, I.-S. Bae, and J.-M. Cha, "Distribution reliability evaluation affected by superconducting fault current limiter," in Transmission and Distribution Conference and Exposition: Latin America (T&D-LA), 2010 IEEE/PES, 2010, pp. 398-402.

[36] S. M. R. Tousi and S. Aznavi, "Performance optimization of a STATCOM based on cascaded multi-level converter topology using multi-objective Genetic Algorithm," in Electrical Engineering (ICEE), 2015 23rd Iranian Conference on, 2015, pp. 1688–1693.

[37] Babaei, M., Jafari-Marandi, R., Abdelwahed, S. and Smith, B., 2017, August. Application of STATCOM for MVDC shipboard power system. In Electric Ship Technologies Symposium (ESTS), 2017 IEEE (pp. 142-147). IEEE.

[38] Babaei, M., Jafari-Marandi, R., Abdelwahed, S. and Smith, B., 2017, February. A simulated Annealing-based optimal design of STATCOM under unbalanced conditions and faults. In Power and Energy Conference at Illinois (PECI), 2017 IEEE(pp. 1-5). IEEE.

[39] T. Kataoka and H. Yamaguchi, "Comparative study of transformer-type superconducting fault current limiters considering magnetic saturation of iron core," Magnetics, IEEE Transactions on, vol. 42, pp. 3386-3388, 2006.

[40] Rostaghi-Chalaki, Mojtaba, A. Shayegani-Akmal, and H. Mohseni. "HARMONIC ANALYSIS OF LEAKAGE CURRENT OF SILICON RUBBER INSULATORS IN CLEAN-FOG AND SALT-FOG." 18th International Symposium on High Voltage Engineering. 2013.

[41] Rostaghi-Chalaki, Mojtaba, A. Shayegani-Akmal, and H. Mohseni. "A STUDY ON THE RELATION BETWEEN LEAKAGE CURRENT AND SPECIFIC CREEPAGE DISTANCE." 18th International Symposium on High Voltage Engineering (ISH 2013). 2013.

[42] Rahimnejad, A., and M. Mirzaie. "Optimal corona ring selection for 230 kV ceramic I-string insulator using 3D simulation." International Journal of Scientific & Engineering Research 3.7 (2012): 1-6.

[43] Akbari, Ebrahim, Mohammad Mirzaie, Abolfazl Rahimnejad, and Mohammad Bagher Asadpoor. "Finite Element Analysis of Disc Insulator Type and Corona Ring Effect on Electric Field Distribution over 230-kV Insulator Strings." International Journal of Engineering & Technology 1, no. 4 (2012): 407-419.

[44] H. Gaztanaga, I. Etxeberria-Otadui, D. Ocnasu, and S. Bacha, "Real-time analysis of the transient response improvement of fixed-speed wind farms by using a reduced-scale STATCOM prototype," Power Systems, IEEE Transactions on, vol. 22, pp. 658-666, 2007.

[45] A. Murdoch, J. Winkelman, S. Javid, and R. Barton, "Control design and performance analysis of a 6 MW wind turbine-generator," Power Apparatus and Systems, IEEE Transactions on, pp. 1340-1347, 1983.

[46] P. Anderson and A. Bose, "Stability simulation of wind turbine systems," Power Apparatus and Systems, IEEE transactions on, pp. 3791-3795, 1983.

[47] B. Adkins and R. G. Harley, The general theory of alternating current machines: Springer, 1975.

[48] A. Foroush Bastani, Z. Ahmadi, D. Damircheli, A Radial basis collocation method for pricing American options under regime-switching jump-diffusion models, Appl. Numer. Math. 65, 79–90, 2013.

[49] A. Foroush Bastani, D. Damircheli An adaptive algorithm for solving stochastic multi-point boundary value problems, Numerical Algorithms 74 (4), 1119-1143, 2017.